

MESHLESS NATURAL NEIGHBOUR METHOD AND ITS APPLICATION IN ELASTO-PLASTIC PROBLEMS

H.H. Zhu, Y.B. Miao and Y.C. Cai

*Department of Geotechnical Engineering, School of Civil Engineering, Tongji University,
200092, P. R. China*

Abstract The meshless natural neighbour method (MNNM) is a truly meshless method, which does not need the Delaunay tessellation of the whole domain to construct the Laplace interpolation. At the same time, some difficulties in other meshless methods, such as the imposition of essential boundary conditions, the treatment of material discontinuities and the choice of weight functions are avoided. The governing equations of elasto-plastic for MNNM are obtained to apply the MNNM to the analysis of two-dimensional elasto-plastic problems. The numerical results indicate that the theory and programmes are accurate and effective.

Keywords: meshless, natural neighbour, natural element, elasto-plastic analysis.

1. INTRODUCTION

Meshless methods are newly developed numerical methods in the last decade. As the approximation/interpolation functions are constructed in terms of scattered nodes, they do not need any mesh structures in the formulation. Because of the mesh-free property, some problems brought by mesh generation, mesh distortion and mesh motion are avoided. More and more engineers and computational mechanics researchers have paid their attentions to this kind of methods.

According to the definition of the shape functions, meshless methods can be mainly grouped into three classes: meshless methods based on kernel function approximation [1–4,], meshless methods based on least square approximation [5–13], and meshless methods based on natural neighbour interpolation [14–20]. In addition, there are some more general meshless methods such as

meshless method based on collocation with radial basis function developed by Zhang *et al.* [21]. They are not ranged into the classification, but the aforementioned three types of meshless methods can be deduced from them.

The representative method of the first class of meshless methods is the Smooth Particle Hydrodynamics (SPH) [1], which was proposed by Lucy and Gingold in 1977. This method has high computational efficiency, but as a result of collocation method used in the discretization of equilibrium equation, the solution of SPH is instable. To improve the stability of SPH, Liu *et al.* developed a modified kernel function method, the Reproducing Kernel Particle Method (RPKM) [2].

The family of meshless methods based on least square approximation has the most members, which is represented by the Element-free Galerkin Method (EFG) developed by Belytschko *et al.* [5]. The family also includes the Finite Point Method (FPM) [9], Hp Clouds method [10], and Local Boundary Integral Equation method (LBIE) [11] etc. These methods have better compatibility and stability. But due to more time consuming, this kind of methods are not so preferable as SPH-like methods in nonlinear large deformation analysis field.

The above-mentioned two classes of methods are the most popular meshless methods at present. Compared to conventional numerical methods (such as FEM), they have many advantages. Unfortunately, many difficulties arise in the computational time, the enforcement of boundary conditions and the treatment of discontinuities, which limit the research within theoretic scope.

The third type of meshless methods are based on the natural neighbour concept to define the shape function. The representative one is Natural Element Method (NEM) proposed by Braun and Sukumar [13, 14]. By constructed in meshless way, the natural neighbour shape function shares several advantages of the FEM, thus avoids the drawbacks of the previous meshless methods. However, the Delauney tessellation of the distinct points in the whole analysis region is needed to construct the natural neighbour shape function, NEM can hardly be recognized as a meshless method. There are fewer research papers about NEM, and it is not as well known as some other meshless methods, such as EFG and SPH.

Recently, a truly meshless method, Meshless Natural Neighbour Method (MNNM) was proposed by our research group. This method adopts the means similar to EFG to seek the natural neighbour points of the integral points and the Delaunay tessellation of the whole region is avoided consequently. Therefore, its shape function takes full advantages of natural neighbour shape function and almost all the advantages of EFG. The objective of the present work is to apply the MNNM to the analysis of two-dimensional elasto-plastic problems. The governing equations of elasto-plastic for MNNM are described, and results of several standard examples are compared with FEM or analytical solutions to verify this.

2. THEORY OF MESHLESS NATURAL NEIGHBOUR METHOD

2.1 Search for natural neighbours

In order to solve the differential equations of boundary value problems in MNNM, a set of distinct nodes $N = \{n_1, n_2, \dots, n_m\}$ should first be set up at the arbitrary geometry shape of domain Ω (see Figure 1).

Suppose that sample point $p(x)$ is an arbitrary numerical integral point of domain Ω , the algorithm for the neighbour-search in MNNM is based on the locally Delaunay triangles. Let the initial influence nodes $M = \{m_1, m_2, \dots\}$ of the point p be confined within the dashed lines of the square as shown in Figure 2.

The next step is to directly determine the natural neighbours of the point p by using the empty circumcircle criterion—if $DT(n_I, n_J, n_K)$ is any Delaunay triangle of the nodal set N , then the circumcircle of DT contains no other nodes of N . Find the node 1 which is the nearest to the sample point p from the nodal set M . Starting with edge $p - 1$ and using the empty circumcircle criterion, we form a set of locally defined triangles $\{p, 1, 2\}, \{p, 2, 3\}, \{p, 3, 4\}, \{p, 4, 5\}$, and $\{p, 5, 6\}$, where the nodes 1–6 are selected from the nodal set M in Figure 2. Now, the nodes 1–6 are just the natural neighbours of the point p .

The natural neighbours of the given point p are unique after the nodal set N has been set up at the domain Ω . The size of the square edges $2r$ in Figure 1 will not and cannot influence the definition of the natural neighbours of point p . The purpose of the restriction of the influence nodes to the square region is to reduce the time for searching for the natural neighbours. Hence, the size of

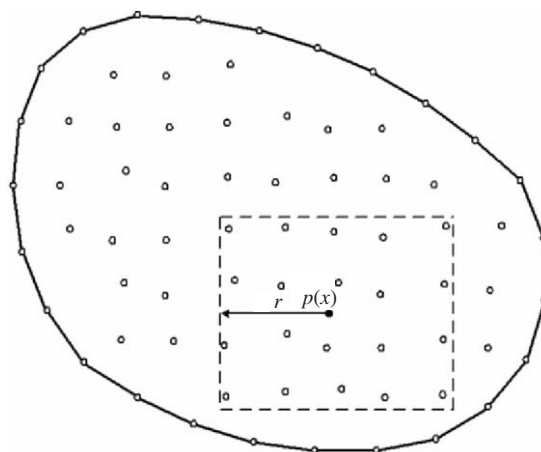


Figure 1. Discrete model of region Ω and its arbitrary integrate point $p(x)$.

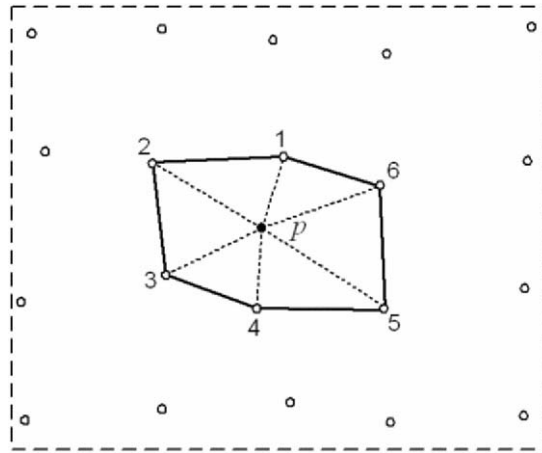


Figure 2. Natural neighbour of the point p .

the length r must be large enough to contain all the natural neighbours of point p , and should be small enough to save the time consume of the neighbour-search. Of course, the nodal set N of domain Ω can be regarded as the initial influence nodal set M of the point p , but the neighbour-search will be much more expensive and can not be afforded.

2.2 Laplace interpolation

Natural neighbours provide a means to define a robust approximation for scattered nodes in Ω according to the relative spatial density and position of nodes. Silbson and Laplace (non-silbson) natural neighbour interpolations are differently used in NEM and NNM. In 2D, the Laplace shape function defined by the ration of length measures [16], whereas the Silbson shape function is based on the ration of areas [14]. The computational cost and algorithm are more favorable in Laplace interpolant than in Silbson interpolant. In this paper, we choose Laplace interpolant to develop the MNNM.

In Figure 3, C_{12p} , C_{23p} , C_{34p} , C_{45p} , and C_{61p} are the circumcentres of the triangles $\{p, 1, 2\}$, $\{p, 2, 3\}$, $\{p, 3, 4\}$, $\{p, 4, 5\}$, and $\{p, 5, 6\}$, respectively. Connecting the points $\{C_{12p}, C_{23p}, C_{34p}, C_{45p}, C_{61p}\}$ by sequence, we can form the voronoi cell of the point p . If the point $p(\mathbf{x})$ has n natural neighbours (6 neighbours in Figure 3), then the Laplace shape function for node i is defined as:

$$\phi_i(\mathbf{x}) = \frac{\alpha_i(\mathbf{x})}{\sum_{j=1}^n \alpha_j(\mathbf{x})}, \alpha_j(\mathbf{x}) = \frac{s_j(\mathbf{x})}{h_j(\mathbf{x})}, \mathbf{x} \in R^2 \quad (1)$$

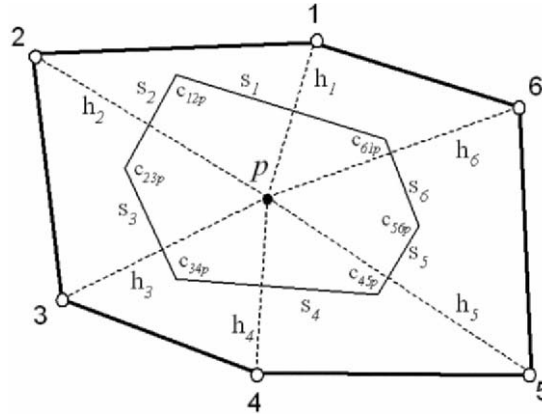


Figure 3. Computation of Laplace interpolation of the natural neighbours.

Where $\alpha_j(\mathbf{x})$ is the Laplace weight function, $s_j(\mathbf{x})$ is the length of the voronoi edge associated with point p and node i , and $h_j(\mathbf{x})$ is the Euclidean distance between point p and node i (Figure 3).

The derivatives of the coordinates are obtained by differentiating Equation (1):

$$\Phi_{i,j}(\mathbf{x}) = \frac{\alpha_{i,j}(\mathbf{x}) - \Phi_i(\mathbf{x})\alpha_{,j}(\mathbf{x})}{\alpha(\mathbf{x})},$$

$$\alpha(\mathbf{x}) = \sum_{k=1}^n \alpha_k(\mathbf{x}), \alpha_{,j}(\mathbf{x}) = \sum_{k=1}^n \alpha_{k,j}(\mathbf{x}) \quad (2)$$

The global forms of displacement approximations $\mathbf{u}^h(\mathbf{x})$ of point $p(\mathbf{x})$ can be written as

$$\mathbf{u}^h(\mathbf{x}) = \sum_{i=1}^n \phi_i(\mathbf{x})\mathbf{u}_i \quad (3)$$

where \mathbf{u}_i ($i = 1, \dots, n$) are the vectors of nodal displacements at the n natural neighbours of point p , and $\Phi_i(\mathbf{x})$ are the shape functions associated with each node.

By defining of the shape function given in Equation (1), the following properties are self-evident.

$$\sum_{i=1}^n \Phi_i(\mathbf{x}) = 1 \quad \mathbf{x} \in \Omega \quad (4)$$

$$\begin{cases} 0 \leq \Phi_i(\mathbf{x}) \leq 1 \\ \Phi_i(\mathbf{x}_j) = \delta_{ij} \end{cases} \quad \mathbf{x} \in \Omega \quad (5)$$

From Equation (5), it can be seen that the Laplace interpolation passes through the nodal values, which is in contrast to most meshless approximations, where the nodal parameters \mathbf{u}_i are not nodal displacements. Also, the Laplace shape function is C^0 at nodal locations as well as on the boundary of the support. These properties make the Laplace interpolant the only meshless data interpolation that will exactly satisfy the (linear) essential boundary conditions. A more detailed discussion of the Laplace interpolation and its application to PDEs can be found in Sukumar *et al.* [16] and the references therein.

It is noted that if the position of the point p is the same as an arbitrary node i , the algorithm in Equation (1) will fail because of the Euclidean distance $h_j(\mathbf{x}) = 0$ and the Laplace weight function $\alpha_i(\mathbf{x}) = \pm\infty$. This situation never arises when the triangular finite elements are used as integral cell so that all integration points are interior to the triangles. But when the regular cells similar to the EFG method are used to the integral scheme, this computational difficulty is encountered. A generally applicable method to overcome this numerical difficulty is to randomly move nodes by a small distance (e.g. $1e-10$) before computing.

3. THE INCREMENT METHOD FOR ELASTO-PLASTIC ANALYSIS

When the elasto-plastic material has reached the plastic state, the stress-strain relationship is,

$$\{d\sigma\} = [D]_{ep}\{d\varepsilon\} \quad (6)$$

This relationship is nonlinear. The step-up loading method can be chosen to linearize the nonlinear problem. At a certain stress and strain level, another loading will produce stress increment $\{\Delta\sigma\}$ and strain increment $\{\Delta\varepsilon\}$. As long as the incremental load is small enough, the Equation (6) can be expressed approximately as follows,

$$\{\Delta\sigma\} = [D]_{ep}\{\Delta\varepsilon\} \quad (7)$$

in which $[D]_{ep}$ is elasto-plastic matrix, e.g., $[D]_{ep} = [D]_e - [D]_p$, which is only dependent on the stress level at the beginning of loading.

The common solution methods of elasto-plastic problem include incremental tangent stiffness method, incremental initial stress method and incremental initial strain method. As the time consume is longer than conventional finite element method, the incremental initial stress method is used in this paper to avoid generating and decomposing of the stiff matrix in every iterate step. In

this way, the stiff matrix which is generated and decomposed at the beginning of solution, can maintain unchanged in the subsequent increments.

4. DISCRETE EQUATIONS

We consider the two-dimensional problem with small displacements on the domain Ω bounded by Γ . The equilibrium equation and boundary conditions are given as follows:

$$\nabla \cdot \boldsymbol{\sigma} + \mathbf{b} = 0, \quad \text{in } \Omega \tag{8a}$$

$$\boldsymbol{\sigma} \cdot \mathbf{n} = \bar{\mathbf{t}}, \quad \text{on } \Gamma_t \tag{8b}$$

$$\mathbf{u} = \bar{\mathbf{u}}, \quad \text{on } \Gamma_u \tag{8c}$$

where $\boldsymbol{\sigma}$ is the stress tensor which corresponds to the displacement filed \mathbf{u} ; \mathbf{b} is the body force vector; the superposed bar in Equations (8b) and (8c) denotes prescribed boundary values, and \mathbf{n} is the unit normal to the domain.

The variational form of Equation (8) is posed as follows

$$\int_{\Gamma_t} \delta u \cdot t \mathbf{d}\Gamma - \int_{\Omega} \delta \boldsymbol{\varepsilon} \cdot \boldsymbol{\sigma} d\Omega + \int_{\Omega} \delta u \cdot b \mathbf{d}\Omega = 0 \quad \forall \delta u \in H_0^1 \tag{9}$$

The discretized system can be obtained by substituting Equation (1) into (9)

$$K \cdot D = f \tag{10}$$

where

$$K_{\mathbf{I}\mathbf{J}} = \int_{\Omega} B_{\mathbf{I}}^T \cdot DE \cdot B_{\mathbf{J}} \mathbf{d}\Omega \tag{11}$$

$$\mathbf{f}_{\mathbf{I}} = \int_{\Gamma_t} \Phi_{\mathbf{I}} \cdot t \mathbf{d}\Gamma + \int_{\Omega} \Phi_{\mathbf{I}} \cdot b \mathbf{d}\Omega \tag{12}$$

where DE is the elasticity matrix, B_I is the strain matrix.

From the above deduction, we can know that the numerical results obtained by NNM [16] and the proposed MNNM are the same because the algorithm for the neighbour-search is the only difference in NNM and MNNM.

5. NUMERICAL EXAMPLES

The MNNM is coded in standard C++. Cases are run in order to examine the MNNM in two-dimensional elastostatics.

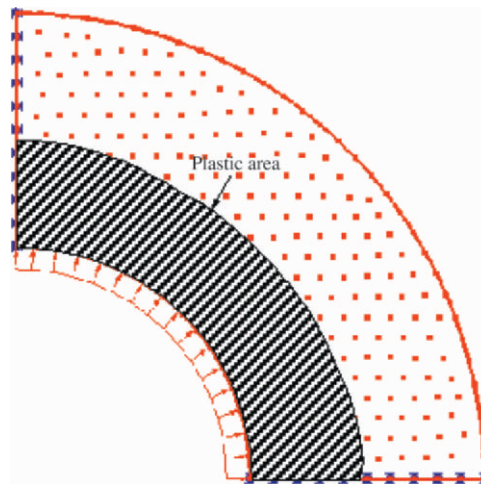


Figure 4. Computational model and plastic area.

5.1 Thick cylinder

Consider an axially restrained thick cylinder of inside diameter $a = 10$ mm, and outside diameter $b = 20$ mm, which is subjected to internal pressure $p = 12$ kPa. The material is perfectly elasto-plastic with Young's modulus $E = 85570$ kPa and Poisson's ratio $\mu = 0.3$. The Von-Mises yield criterion is adopted and the tensile yield limit σ_s is equal to 10 kPa. The problem statement is given in Figure 4.

The comparison in Figures 5 and 6 show that, with the same nodes distribution, the results obtained by MNNM are in good agreement with the analytical solutions and much better than those obtained by triangular FEM.

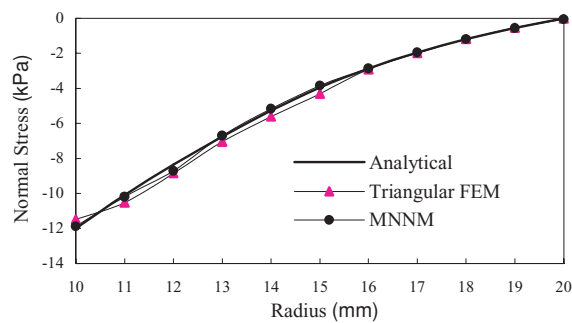


Figure 5. Comparison of normal stress.

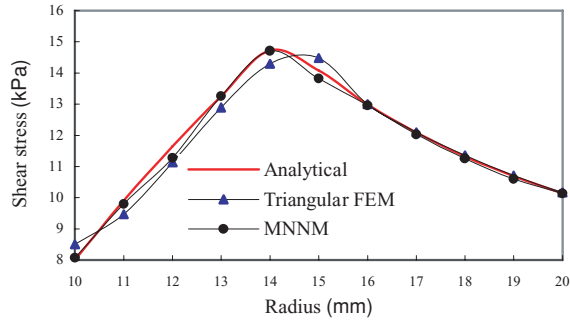


Figure 6. Comparison of shear stress.

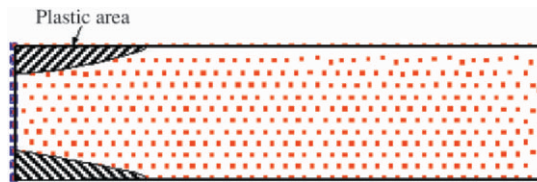


Figure 7. Computational model and plastic area for cantilever beam problem.

5.2 Cantilever beam

The second example considered here is a rectangle cantilever beam of length $l = 40\text{ m}$ and height $h = 10\text{ m}$ as shown in Figure 7. The beam is fixed at one end and subjected to concentrated load $P = -11\text{ kN}$ at the free end. The material is perfectly elasto-plastic and obeys the Von-Mises yield criterion. The material parameters are $E = 86670\text{ kPa}$, $\mu = 0.3$ and $\sigma_s = 10\text{ kPa}$. With the same nodes distribution, the comparison of σ_x , the normal stress in x direction, is shown in Figure 8.

6. CONCLUSION

The Meshless Natural Neighbour Method, which is a truly meshless method similar to EFG, can treat material discontinuities conveniently and keep some advantages of FEM. In this paper, by combining MNNM and incremental initial stress method, a general C++ programme has been worked out and applied into elasto-plastic analysis, in which perfectly elasto-plastic model and Von-Mises yield criterion is adopted. Although only several simple examples were presented in this chapter, it is expected that the proposed method can be used to solve some more complicated problems in geotechnical engineering,

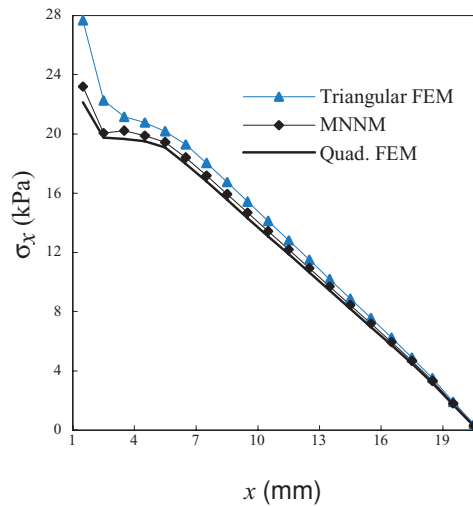


Figure 8. Comparison of σ_x

as well as problems with large deformation such as landsliding and pile penetration.

REFERENCES

1. R.A. Gingold and J.J. Moraghan (1977), Smoothed particle hydrodynamics: theory and applications to non-spherical stars. *Monthly Notices of the Royal Astronomical Society*, 181, 2, pp. 375–389.
2. W.K. Liu, S. Jun and Y.F. Zhang (1995), Reproducing kernel particle methods. *International Journal for Numerical Methods in Fluids*, 20, pp. 1081–1106.
3. W.K. Liu and Y. Chen (1995), Wavelet and multiple scale reproducing kernel method. *International Journal for Numerical Methods in Fluids*, 21, pp. 901–931.
4. R.R. Ohs and N.R. Aluru (2001), Meshless analysis of piezoelectirc devices. *Computational Mechanics*, 27, pp. 23–36.
5. T. Belytschko, Y.Y. Lu and L. Gu (1994), Element-free Galerkin method. *International Journal for Numerical Methods in Engineering*, 37, pp. 229–256.
6. B. Nayroles, G. Touzot and P. Villon (1992), Generalizing the finite element method: diffuse approximation and diffuse elements. *Computational Mechanics*, 10, pp. 307–318.
7. L.W. Cordes and B. Moran (1996), Treatment of material discontinuity in the Element-free Galerkin method. *Computer Methods in Applied Mechanics and Engineering*, 139, pp. 75–89.
8. Y. Krongauz and T. Belytschko (1998), EFG approximation with discontinuous derivatives. *International Journal for Numerical Methods in Engineering*, 41, pp. 1215–1233.
9. E. Oñate, S.R. Idelsohn, O.C. Zienkiewicz et al. (1996), A finite point method in computational mechanics: applications to convective transport and fluid flow. *International Journal for Numerical Methods in Engineering*, 39, pp. 3839–3866.

10. C.A. Duarte and J.T. Oden (1996), Hp clouds: a h-p meshless method. *Numerical Methods for Partial Differential Equations*, 12, pp. 673–705.
11. T. Zhu, J. Zhang and S.N. Atluri (1998), A local boundary integral equation (LBIE) method in computational mechanics, and a meshless discretization approach. *Computational Mechanics*, 21, pp. 223–235.
12. S.N. Atluri and T. Zhu (1998), A new meshless local Petrov-Galerkin (MLPG) approach in computational mechanics. *Computational Mechanics*, 22, pp. 117–127.
13. J. Braun and M. Sambridge (1995), A numerical method for solving partial differential equations on highly irregular evolving grids. *Nature*, 376, pp. 655–660.
14. N. Sukumar, B. Moran and T. Belytschko (1998), The nature element method in solid mechanics. *International Journal for Numerical Methods in Engineering*, 43, pp. 839–887.
15. E. Cueto, M. Doblare and L. Gracia (2000), Imposing essential boundary conditions in the natural element method by means of density-scaled α -shapes. *International Journal for Numerical Methods in Engineering*, 49, pp. 519–546.
16. N. Sukumar, B. Moran and Y. Semenov (2001), Natural neighbour Galerkin method. *International Journal for Numerical Methods in Engineering*, 50, pp. 1–27.
17. N. Sukumar (2003), Voronoi cell finite difference method for the diffusion operator on arbitrary unstructured grids. *International Journal for Numerical Methods in Engineering*, 57, pp. 1–34.
18. S.R. Idelsohn, E. Oñate, N. Calvo and F.D. Pin (2003), The meshless finite element method. *International Journal for Numerical Methods in Engineering*, 58, pp. 893–912.
19. E. Cueto, N. Sukumar, B. Calvo, M.A. Martínez, J. Cegoñino and M. Doblare (2003), Overview and recent advances in natural neighbor Galerkin methods. *Archives of Computational Methods in Engineering*, 10, 4, pp. 307–384.
20. Y.C. Cai and H.H. Zhu (2004), A meshless local natural neighbour interpolation method for stress analysis of solids. *Engineering Analysis with Boundray Elements*, 28, 6, pp. 607–613.
21. X. Zhang, K.Z. Song, M.W. Lu *et al.* (2000), Meshless methods based on collocation with radial basis function. *Computational Mechanics*, 26, 4, pp. 333–343.